

1 **Overlapping transcriptional expression response of wheat zinc-induced**
2 **facilitator-like transporters emphasize important role during Fe and Zn stress**

3

4 Shivani Sharma^{1,2} (Email: shivanisharma.mtech2012@gmail.com), Gazaldeep Kaur¹ (Email:
5 gazaldeep.gk@gmail.com), Anil Kumar¹ (Email: anilkumar0919@gmail.com), Jaspreet Kaur²
6 (Email: jaspreet_uiet@pu.ac.in) and Ajay Kumar Pandey¹ (Email: pandeyak@nabi.res.in)

7

8 **Author affiliations**

9 ¹National Agri-Food Biotechnology Institute (Department of Biotechnology), Sector 81,
10 Knowledge City, Mohali, Punjab, India-140306.

11 ²University Institute of Engineering and Technology, Sector 25, Panjab University, Chandigarh,
12 Punjab, India-160015

13

14 *Corresponding author

15 Dr. Ajay K Pandey, Scientist-E

16 National Agri-Food Biotechnology Institute (Department of Biotechnology), Sector 81,
17 Knowledge City, Mohali-140306, Punjab, India.

18 Telephone: +91-1724990124

19 Email: pandeyak@nabi.res.in; pandeyak1974@gmail.com

20 **ORCID ID: 0000-0003-1064-139X**

21 **Acknowledgments**

22 The authors thank Executive Director, NABI for facilities and support. This research was funded
23 by the NABI-CORE grant to AKP. Thanks to the International Wheat Genome Sequencing
24 Consortium for providing the high-quality wheat genome resources.

25

26 **Abstract**

27 **Background**

28 Hexaploid wheat is an important cereal crop that has been targeted to enhance grain
29 micronutrient content including zinc and iron. In this direction, modulating the expression of
30 plant transporters involved in Fe and Zn homeostasis could be one of the promising approaches.
31 Therefore, the present work was undertaken to identify bread wheat Zinc-Induced Facilitator-
32 Like (ZIFL) family of transporters and study their transcriptional expression response during
33 micronutrient fluctuations and exposure to multiple heavy metals.

34 **Results**

35 The genome-wide analyses resulted in identification of thirty-five putative *TaZIFL* genes, which
36 were distributed only on Chromosome 3, 4 and 5. Wheat ZIFL proteins subjected to the
37 phylogenetic analysis showed the uniform distribution along with rice, *Arabidopsis* and maize.
38 *In-silico* analysis of the promoters of the wheat ZIFL genes suggested the presence of multiple
39 metal binding sites including those which are involved in Fe homeostasis. QRT-PCR analysis of
40 wheat *ZIFL* genes suggested the differential regulation of the transcripts in roots and shoots
41 under surplus Zn and also during Fe starvation. Specifically, in roots, *TaZIFL2.3*, *TaZIFL4.1*,
42 *TaZIFL4.2*, *TaZIFL5*, *TaZIFL6.1* and *TaZIFL6.2* were significantly up-regulated by both Zn and
43 Fe. This suggested that ZIFL could possibly be regulated by both the nutrient stress in a tissue

44 specific manner. Interestingly, upon exposure to heavy metals, *TaZIFL4.2* and *TaZIFL7.1*
45 showed significant up-regulation, whereas *TaZIFL5* and *TaZIFL6.2* remained almost unaffected.

46 **Conclusion**

47 This is the first report with detailed analysis of wheat ZIFL genes. Our study also identifies
48 closest ortholog for transporter of mugineic acid, a chelator required for Fe uptake.

49 Comprehensive transcript expression pattern during development of wheat seedlings and against
50 various abiotic/biotic stresses resulted in tissue specific responses. Overall, this work addresses
51 the role of wheat *ZIFL* during the interplay between micronutrient and heavy metal stress in a
52 tissue specific manner.

53 **Keywords:** iron starvation, micronutrient uptake, *Triticum aestivum* L., zinc transport,
54 biofortification

56 **Background**

57 Crop plants are an important target for enhancing micronutrient content, including iron (Fe) and
58 zinc (Zn) in the developing grains. From human nutritional point of view, these micronutrients
59 play an important role in growth and development, cognitive and immune impairment, and in
60 gene regulation (Nyaradi et al., 2013; Gibson et al., 2018; Wishart et al., 2017). Therefore,
61 researches worldwide are identifying diverse approaches to generate micronutrient rich food
62 crops. Apart from a nutritional point of view, Fe and Zn are also essential minerals for plant
63 development and various biochemical functions (Rout et al., 2015; Hafeez et al., 2013). Multiple
64 metal specific transporters and regulators show co-expression and could share common signaling
65 features including the response towards Zn, Fe or other metals. Several specific transporters are
66 involved in the uptake and translocation of Fe and Zn, inside the plant has been described

67 previously (Kawachi et al., 2018; Stein et al., 2009; Klein et al., 2009; Eide et al., 2014; Lee et
68 al.,2009; Morrissey et al., 2009; Morel et al., 2008). Efficient micronutrient uptake by plants is a
69 concerted effort of major genes belonging to the different families of transporters that include,
70 but are not limited to zinc–regulated transporter, iron–regulated transporter family, the natural
71 resistance associated macrophage protein family, yellow-stripe 1-like (YSL) subfamily of the
72 oligopeptide transporter superfamily, Ca²⁺-sensitive cross complementer 1 (CCC1) family
73 (Yoneyama et al., 2015; Ishimaru et al.,2011; Romheld et al., 2004; Sinclair et al.,2012; Kumar
74 et al., 2018).

75 Many evidences are gathering that suggest an important role of major facilitator
76 superfamily (MFS) clan of transporters, yet the identification of specific candidate genes has
77 been always a bottleneck. Earlier, one such important group of genes referred as Zinc-induced
78 facilitator-1 like gene (*ZIFL*), was identified and its role was assessed in different stresses
79 including Zn homeostasis (Haydon et al., 2007). Role of *ZIFL* was not addressed in crop plants
80 until the reports describing the inventory from model plant *Arabidopsis thaliana* and crop like
81 *Oryza sativa* came forth (Haydon et al.,2007; Ricachenevsky et al., 2011). Since, the first
82 identification of the three *ZIFL* in *Arabidopsis* referred to as *AtZIF1* (AT5G13740), *AtZIFL1*
83 (AT5G13750) and *AtZIFL2* (AT3G43790) evidences are accumulating for their role specifically
84 in Zn homeostasis (Haydon et al., 2007). Subsequently, multiple *ZIFLs* from monocot such as
85 rice were identified and the presence of high numbers of these genes was correlated with the
86 genome duplication events. Further, it was speculated that plant *ZIFLs* might perform redundant
87 function that is imperative by their overlapping expression response for Fe and Zn (Haydon et
88 al., 2012). In addition to that rice *ZIFL* family of genes were also characterized to be transporter
89 of mugineic acid, a phytosiderophores involved in strategy-II mode of Fe uptake via roots

90 (Nozoye et al.,2011; Nozoye et al., 2015). Recently, ZIFL1.1 in *Arabidopsis* was shown to
91 impact the cellular auxin efflux at the root tip and contribute for drought tolerance (Remy et al.,
92 2013). Furthermore, the role of ZIFLs was expanded for their involvement in potassium
93 homeostasis and their ability to transport transition metal like cesium. (Remy et al., 2013).
94 Subsequently, the maize (*Zea mays*) Zm-mfs1 was also identified and characterized. (Simmons
95 et al., 2003). Such studies provide a valuable clue to the importance of ZIFL that is not just
96 limited to transport of important micronutrients.

97 Hexaploid wheat (*Triticum aestivum* L.) is an important crop for the developing countries
98 where, the suboptimal levels of grain Zn and Fe have been reported. Initiatives to enhance
99 multiple micronutrients including Zn and Fe are being undertaken by either gain of function
100 approach or RNAi mediated gene silencing (Connorton et al., 2017; Singh et al., 2017; Aggarwal
101 et al., 2012). Earlier, using wheat grain transcriptome data it was confirmed that a higher
102 proportion of transcripts were present in abundant amount that are known to be involved in
103 transport activity (GO:0005215) (Gillies et al., 2012). Therefore, such studies provided the
104 framework to investigate new resources and genes that could be of immense value to address the
105 uptake and remobilization of micronutrients in cereal grains such as wheat. To provide impetus
106 in this direction, the inventory of wheat ZIFL was built and their detailed expression
107 characterization was performed.

108 In the current work, thirty-five wheat (*Triticum aestivum* L.) putative ZIFL proteins were
109 identified that show their restricted distribution only on three chromosomes viz. 3, 4 and 5.
110 Phylogenetic analysis revealed a uniform distribution of wheat ZIFL sequences in multiple
111 clades along with rice, *Arabidopsis* and *Z. mays*. Detailed characterization of the *ZIFL* genes for
112 their motif composition, promoter sequences and their expression under Fe limiting and Zn

113 surplus condition and other heavy metals was also performed. Our data indicate that the wheat
114 ZIFL show overlapping expression response during Fe starvation and Zn excess condition. Few
115 of the wheat ZIFL gene expression remained unaffected by the presence of heavy metals.
116 Overall, characterization of crop ZIFL transporters could result in identifying specific
117 candidate/s that could be used further to modulate specific Fe-Zn uptake in crop plants such as
118 wheat.

119

120 **Results**

121 **Inventory of wheat ZIFL and their phylogeny analysis**

122 In order to identify wheat *ZIFL* genes and to gain insight for possible evolutionary relationship,
123 two complementary approaches were used. This includes, first performing genome-wide
124 sequences of MFS_1 family using Pfam (PF07690) search, followed by homology-based
125 analysis with previously reported *ZIFL* genes in different plant species Ensembl database. These
126 approaches resulted in the identification of one hundred seventy-nine sequences and to further
127 validate their identity sequences were checked and searched for a MFS_1 domain through Pfam
128 and conserved domain databases (CDD-NCBI) (Table S2). These sequences were then used to
129 build phylogenetic tree with previously known ZIFL proteins sequences from different plants
130 (Table S1 and Figure S1). The arrangement of tree suggested a distinct clade for the ZIFL
131 clustered when compared to the remaining MSF_1 proteins. This indicates that ZIFL is a distinct
132 group of MFS transporters that are tightly clustered (Figure S1). Further, this distribution was
133 validated through two signature sequences that are specific to ZIFLs (i) W-G-x(3)-D-[RK]-x-G-
134 R-[RK] (except in TaZIFL2.5-5D) (ii) S-x(8)-[GA]-x(3)-G-P-x(2)-G-G with an exception of A
135 instead of G at 10th position of (ii) signature in TaZIFL2. Furthermore, sequences similar to ZIFL

136 specific cysteine (Cys) and histidine (His) signatures were also used for identifying TaZIFLs.
137 (iii) C-[PS]-G-C, absent in 5 TaZIFLs (TaZIFL2, TaZIFL 5-5D, TaZIFL 3-4B, TaZIFL 5-5D,
138 TaZIFL 7.1-4B, TaZIFL 7.2-4B) probably due to missing sequence information and (iv) [PQ]-E-
139 [TS]-[LI]-H-x-[HKLRD] (an insertion of ETLYCRHEHRYSIFISLD sequence within the motif
140 was found in TaZIFL7.2-4A) (Ricachenevsky et al., 2011). The presence of one or another ZIFL
141 signature motif further validated the distribution of genes. These signatures guided identification
142 of specific wheat ZIFLs from the rest of the MFS_1 members. Such analysis resulted in
143 confirmation of a total of thirty-five wheat ZIFL sequences, including individual *TaZIFL* genes
144 and their respective homoeologs from different wheat sub-genomes (Table S3). To check the
145 distribution along with other plant species, ZIFL protein sequences from *O. sativa*, *Z. mays* and
146 *Arabidopsis* were used to build a rooted phylogenetic tree through the NJ method (Figure 1).
147 Because of the genome duplication events in wheat, the genes are likely to show multiple alleles
148 of a single gene. Hence the resulted thirty-five putative wheat *ZIFLs* represent 15 genes after
149 distribution of their respective homoeologous (Figure 1). To provide the uniform nomenclature,
150 *TaZIFL* genes were named according to their respective closest known orthologs from rice.
151 Among the wheat ZIFL proteins TaZIFL4.1 showed highest homology with TaZIFL4.2 of 95.2
152 percentage identity. When a cross species comparison was done, the maximum identity of 87
153 percent was shown by TaZIFL2.2-3D and AtZIFL2. With rice, the highest percentage identity of
154 87 was observed for wheat ZIFL2.2-3A and OsZIFL2. The divergence was observed
155 among TaZIFL3-4B and OsZIFL13 with percentage identity of 50.

156

157 **Molecular structure and genome organization**

158 The predicted protein length of the identified wheat ZIFL sequence ranged from 300 to 562
159 amino acids (Table S2). In general, most of the wheat ZIFL showed 10-12 predicted trans-
160 membrane (TM) domains as reported in rice [19]. Specifically, 16 wheat ZIFL proteins were
161 predicted to have 12 TM domains, 15 proteins have 10-11 predicted TM domains, 4 proteins
162 were found to have 8-9 TM domains and only one wheat ZIFL has 4 TM domains (Table S2).
163 Further, the genomic organization, analysis revealed the presence of genes on all three A, B and
164 D sub-genomes. Maximum number of genes were found to be present on B and D sub-genome
165 with 13 and 12 genes respectively (Figure 2a). TaZIFL1.2, TaZIFL2.2, TaZIFL3.4, TaZIFL5,
166 TaZIFL6.2, TaZIFL7.1, TaZIFL7.2 are present in all three genomes, while TaZIFL2.3 and
167 TaZIFL2.4 are present on only one genome 5B and 5D respectively (Table S2). The
168 chromosomal distribution mapping revealed *TaZIFLs* to be present only on chromosome 3, 4 and
169 5 with maximum of 17 sequences on chromosome 4 (Figure 2b and c). Next, the genomic
170 structure was analyzed and regions corresponding to intron-exons were marked (Figure 3).
171 *TaZIFL* clustered into the same group and shared almost similar distribution pattern for the
172 number of exon/intron. The intron-exon number varies from 14-17 in the respective *TaZIFL*
173 genomic sequences (Figure 3, Table S2).

174

175 **Protein motif analysis reveals presence of diverse domains**

176 To have an understanding about the similarity, variation in motif composition and distribution of
177 TaZIFL, 15 sequences representing each ZIFL transcript were subjected to MEME analysis. Our
178 analysis revealed the presence of fifteen motifs (Figure 4a, Table S3). Out of fifteen motifs, six
179 were conserved throughout all ZIFL, while some lacked few motifs. Four unique and exclusively
180 motifs (12, 13, 14, 15) were identified, which are specific to the respective group. Motif 14 and

181 motif 12 (Figure 4b, Table S3) are specific to TaZIFL2.1, TaZIFL2.2, TaZIFL2.3, TaZIFL2.4
182 and TaZIFL2.5, which indicated that TaZIFL2 members might share similar functions. Motif 14
183 was also present in TaZIFL6.2. Another set of unique motifs, mentioned as motif 13 and 15 was
184 found in TaZIFL4.1 and TaZIFL4.2, which may indicate probable different function from rest of
185 TaZIFLs. The canonical MFS signature WG[V/M/I][F/V/A/I]AD[K/R][Y/I/H/L]GRKP was
186 present in the cytoplasmic loop between TM2 and TM3 (Figure S2, Table S4) as well S-x(8)-G-
187 x(3)-G-P-[A/T/G]-[L/I]-G-G as anti porter signature in TM5. The results suggest that ZIFL
188 proteins share unique signatures and high similarity indicating they are a distinct group of MFS
189 family. Presence of conserved signatures Cysteine (Cys) -containing motif CPGC reported
190 previously were also present in most of the wheat ZIFL proteins (Ricachenevsky et al., 2011).
191 The absence of these motifs was observed in TaZIFL2.5_5D, TaZIFL 3_4B, TaZIFL 4.2_4A,
192 TaZIFL5_5D, TaZIFL7.1_4D this might be because of missing sequence information. This motif
193 was found to be present in the cytoplasmic N-terminal loop for TaZIFL groups 2, 4, 5, 6 and in
194 the non-cytoplasmic N-terminal loop for groups 1, 3 and 7 (Figure S2 and Table S4). Another
195 conserved histidine (His)-containing motif PET[L/I]H showed its presence in the cytoplasmic
196 loop between TM domains ranging from 2 and 3 to 6 and 7, with highest between 6 and 7 TM
197 domains (Figure S2).

198

199 **Identification of conserved cis-elements in the promoters of wheat ZIFL genes**

200 To find the molecular clues that could regulate the expression of wheat *ZIFL* transcripts, the 1.5
201 kB promoter region of the all identified wheat *ZIFL* genes was explored. Our analysis revealed a
202 large number of cis-elements in the promoter of wheat ZIFL. Predominantly, the promoters were
203 enriched with the presence of the core binding site for iron-deficiency responsive element

204 binding factor 1 (IDEF), iron related transcription factor 2 (IRO2) and heavy metal responsive
205 element (HMRE) (Table 5). The presence of these promoter elements suggests that wheat *ZIFL*
206 genes might respond towards the presence of heavy metals and to important micronutrients like
207 Fe and Zn. Interestingly, IDE1 cis-element was present on all the promoters of the respective
208 wheat *ZIFL*s suggesting that they could respond to Fe limiting conditions. Few of these
209 promoters consist of multiple such cis-elements suggesting their diverse function in plants (Table
210 S5).

211

212 **Expression characterization of wheat *ZIFL* genes for their response to Zn and Fe**

213 *ZIFL* are primarily known to respond towards Zn excess, therefore experiments were performed
214 to study the gene expression of wheat *ZIFL* in roots and shoots. The QRT - PCR analysis
215 suggested tissue specific expression response by wheat *ZIFL*s. A total of eight genes, including
216 *TaZIFL1.2*, *TaZIFL2.2*, *TaZIFL2.3*, *TaZIFL4.1*, *TaZIFL4.2*, *TaZIFL5*, *TaZIFL6.1* and
217 *TaZIFL6.2* showed significantly higher expression during one of the time points under Zn
218 surplus condition (Figure 5). Of all the genes, the fold expression level for *TaZIFL4.1* was
219 highest (~7 fold) at 3D after treatment with respect to control roots (Figure 5a). In shoots,
220 *TaZIFL1.1*, *TaZIFL1.2*, *TaZIFL6.1* and *TaZIFL6.2* showed significant transcript accumulation
221 either at 3D or 6D after treatment. In our current study, a few genes like *TaZIFL 1.1*, *TaZIFL7.1*
222 and *TaZIFL7.2* remained unaffected by the Zn surplus condition in roots (Figure 5b). Notably,
223 *TaZIFL1.2*, *TaZIFL6.1* and *TaZIFL6.2* show enhanced transcript accumulation in both the
224 tissues. In contrast, during our experiment the expression of a few wheat *ZIFL* genes showed
225 down-regulated in shoots but not in roots. Our expression data under Zn surplus condition
226 suggested the differential response by wheat *ZIFL* towards the treatment.

227 Previous evidences indicated that plant ZIFL genes not only respond to Zn excess, but
228 also are also affected by the Fe limiting conditions (Haydon et al., 2012). Therefore, expression
229 analysis of wheat *ZIFL* genes was checked in roots and shoots of seedling subjected to a Fe
230 limiting condition. Interestingly, in the roots expression of *TaZIFL4.1*, *TaZIFL4.2* and
231 *TaZIFL7.2* show up-regulation during Fe limiting condition at both at 3 and 6 days after
232 starvation. Out of the remaining genes, *TaZIFL2.3*, *TaZIFL6.2* and *TaZIFL7.1* show significant
233 transcript abundance at one-time point or the other (Figure 6a). Interestingly, in shoots
234 *TaZIFL1.1*, *TaZIFL4.1*, *TaZIFL4.2*, *TaZIFL5* and *TaZIFL7.1* show up-regulation only at 3D,
235 suggesting their coordinated response in shoots (Figure 6b). Under –Fe condition, wheat *ZIFL*
236 genes, namely, *TaZIFL4.1* and *TaZIFL4.2* show high transcript accumulation in both roots and
237 shoots. Remaining genes remain unaffected by the Fe stress (Figure 6b). Overall, our expression
238 data suggested that indeed wheat ZIFL respond to the Fe limiting condition, thereby suggesting a
239 common interlink of this gene family during Zn and Fe homeostasis.

240

241 **Putative wheat TOM genes showed expression response in presence of heavy metals**

242 Our promoter analysis of wheat *ZIFL* genes indicates the presence of multiple HMRE suggesting
243 that few of these genes could respond to the heavy metals (Supplementary Table S5).

244 Furthermore, the phylogenetic arrangement of the wheat ZIFL proteins along with the rice
245 suggested the corresponding candidate for the transporter of mugineic acid (TOM). Thus, based
246 on the clade distribution for the corresponding candidate orthologs for the TOM genes for rice
247 (TOM1-OsZIFL4, TOM2-OsZIFL5 and TOM3-OsZIFL2) are identified as
248 *TaZIFL4.1/TaZIFL4.2*, *TaZIFL5*, *TaZIFL6.1*, *TaZIFL6.2*, *TaZIFL7.1*. and *TaZIFL7.2*. Due to
249 the importance of TOM gene in micronutrient mobilization the expression of these transcripts in

250 wheat seedlings (shoots and roots) was studied after exposure to heavy metals such as Co, Ni and
251 Cd. During our experiment all the seedlings showed phenotypic defects when exposed to heavy
252 metals (data not shown). Our expression analysis suggested that wheat ZIFL genes show metal
253 specific responses. For example, *TaZIFL4.2* and *TaZIFL7.1* showed significant up-regulation in
254 both roots and shoots when exposed to any of the metals tested (Figure 7). In contrast, the
255 transcripts of *TaZIFL5* and *TaZIFL6.2* remained unaffected under these heavy metals.
256 Expression of *TaZIFL7.2* showed almost no change in the presence of Ni in either yet it
257 specifically up-regulated in shoots when exposed to Cd or Co. Similarly, *TaZIFL6.1* showed
258 significant upregulation only in roots upon exposure to Ni and Co (Figure 7). Overall, these data
259 indicate the influence of specific heavy metals on the expression of wheat ZIFL genes in a tissue
260 dependent manner.

261

262 **Expression of wheat ZIFL transcripts in different wheat tissues**

263 Analysis of ZIFL genes was also performed in different wheat tissues and developmental stages
264 by using transcript expression data. RNA-seq expression analysis for *TaZIFL* was also checked
265 under different stresses. The expression values were extracted as Transcript per millions (TPM)
266 from a wheat expression browser, expVIP (<http://www.wheat-expression.com/>). *TaZIFL*
267 expression values in different tissues (aleurone-al, starchy endosperm-se, seed coat-sc, leaf, root,
268 spike, shoot) and various developmental stages were extracted (Table S6) and were depicted as a
269 heatmap (Figure 8). In reference to grain tissue developmental time course (GTDT) (Gillies et
270 al., 2012), highest expression was seen for *TaZIFL1.2* (3B, 3D) and *TaZIFL5* (5A, 5B), with an
271 increase in expression in “al” at 20 dpa and “al and se” at 30 dpa. In the expression values during
272 grain tissue specific expression (at 12 dpa) (Pearce et al., 2014), *TaZIFL1.2* was not expressed,

273 but like GTDT study, *TaZIFL5* (5A, 5B) was expressed in “al” as well as “se”. While for sc
274 tissue, *TaZIFL2.2-3D* and *TaZIFL7.1* (4A, 4D) had the highest expression when compared to
275 other *ZIFL* genes. For the tissue specific expression response *TaZIFL2.2* was abundant in spike,
276 *TaZIFL1.2* in leaf and root. *TaZIFL5* was predominantly expressed in all the tested tissue,
277 including leaf, shoot, spike and shoot. The transcripts exclusively expressed in root were
278 *TaZIFL2.4-5D*, *TaZIFL2.5-5B*, *TaZIFL6.1-5A*, and *TaZIFL7.2-4D*, with high induction of
279 *TaZIFL4.1* (4B, 4D), *TaZIFL4.2-4A*, *TaZIFL6.2* (4A, 4B, 4D) for three-leaf and flag leaf stage
280 as compared to the seedling stage. Highest expression induction was seen for *TaZIFL4.2-4D*. In
281 addition, the highest expression overall in five tissues was observed for *TaZIFL1.2* (3A, 3B, 3D)
282 in leaves for seedling as well as tillering stage, *TaZIFL2.2-3D* in spike, *TaZIFL3-4A* in leaf,
283 *TaZIFL5-5A* in grain, *TaZIFL7.1-4D* in grain and leaf.

284 No significant changes in the *TaZIFL* gene expression were observed for *Fusarium* head
285 blight infected spikelets (Table S6, Figure S3). For *Septoria tritici* infected seedlings, while a ~2-
286 fold induction was observed for *TaZIFL1.2* (3A, 3B) after 4 days of induction, prolonged
287 infection (13 days), resulted in its downregulation. Other *ZIFLs* showing changed expression
288 were *TaZIFL1.2-3D* and *TaZIFL2.2-3A* (>2 fold up-regulation), *TaZIFL3-4B* (upto 2.7-fold
289 downregulation). *TaZIFL1.2* (3A, 3B, 3D) were also downregulated (upto ~4 fold) in seedlings
290 with stripe rust infection, while only *TaZIFL1.2-3D* was downregulated under powdery mildew
291 infection. For abiotic stress, while no major changes were observed for *TaZIFLs*, *TaZIFL4.1*
292 (4B, 4D) & *TaZIFL4.2* (4A, 4D) were found to be significantly downregulated by ~14-fold
293 under phosphate starvation, while *TaZIFL6.2-4D* was downregulated by 3-fold (Table S6, Figure
294 S3). Under heat, drought and heat-drought combined stress (Table S6, Figure S3), *TaZIFL7.1*
295 (4A, 4D) and *TaZIFL7.2-4D* were induced by upto ~7-fold and ~2-fold respectively, whereas

296 TaZIFL1.2 (3A, 3B, 3D) and TaZIFL5 (5A, 5B) were downregulated by 6 and 7.5-fold,
297 respectively. These expression data suggest that specific ZIFLs are differentially regulated under
298 infection conditions and show perturbed expression under abiotic stresses.

299

300 **Discussion**

301 **Wheat ZIFL proteins as putative phyto siderophore efflux transporters**

302 The current work was undertaken to build the inventory of wheat ZIFL. Since wheat is a
303 hexaploid species with three genomes therefore, we expect a high number of transcripts encoding
304 for a particular gene family. Our analysis resulted in the identification of a total of thirty-five
305 ZIFL-like genes from hexaploid wheat. A unique observation made for the wheat ZIFLs is that
306 all the genes are restricted to chromosome 3, 4 or 5 only. With the exception of a seven ZIFL
307 genes, rest are localized on all the three homoeologous in the wheat genomes i.e. A, B, and D
308 (Figure 3). This study and the previous preliminary report, led to the identification of a total of
309 fifteen ZIFL with *TaZIFL1.2*, *TaZIFL2.2*, *TaZIFL3*, *TaZIFL4.2*, *TaZIFL5*, *TaZIFL6.2*, *TaZIFL7.1*
310 and *TaZIFL7.2* showing the presence of all the homoeologous (homoalleles) genes (Pearce et al.,
311 2014). All the wheat ZIFLs belongs to the MFS superfamily, thereby containing the canonical
312 ZIFL MFS signature and MFS antiporter sequence (Figure S3). Given the high sequence
313 homology, they are named from TaZIFL1 to TaZIFL7 according to their clad distribution in the
314 phylogenetic tree that corresponds to the rice genes. Previously, in rice multiple TOM genes
315 were identified as protein belonging to the ZIFL sub-family. Subsequent characterization of
316 these rice ZIFL genes led to the identification of functionally active *OsTOM1*, *OsTOM2* and
317 *OsTOM3* (Nozoye et al., 2011; Nozoye et al., 2015). Therefore, based on the phylogenetic
318 arrangement and previous characterization in rice, the corresponding homolog for the putative

319 functional wheat TOM could be *TaZIFL4.1/4.2*, *TaZIFL5* and *TaZIFL7.1/7.2*. Based on our
320 analysis, wheat ZIFL proteins show localization on the PM, except for *TaZIFL4.2-B* and
321 *TaZIFL5-D*. These two wheat ZIFL predicted proteins are putatively localized on vacuolar
322 membrane, thereby making them a strong candidate in a quest to identify novel membrane
323 transporters for micronutrient storage in the cell organelles. In general, very small numbers of
324 *ZIFL* genes are being reported from dicot species like *Arabidopsis* and *Vitis vinifera* and *Populus*
325 *trichocarpa* (Ricachenevsky et al.,2011). Given the complexity of the wheat genome one could
326 certainly anticipate the presence of multiple possible putative phyto siderophore efflux
327 transporters that needs to be functionally characterized in the near future. In rice, the high ZIFL
328 numbers in rice could be accounted due to the lineage-specific expansion of the gene family
329 (Ricachenevsky et al., 2011). Overall, our analysis identified highest number of *ZIFL* genes
330 reported till date from any monocot species.

331

332 **Wheat ZIFL genes display overlapping gene expression**

333 Plants undergoing metal stress result in series of signaling events that largely includes
334 reprogramming of transcripts that could help them to overcome the toxicity. In plants, excess of
335 Zn also results in the generation of reactive oxygen and nitrogen species (Feigl et al., 2015). The
336 abundance of multiple membrane proteins is increased by the presence of either excess Zn or Fe
337 deficiency. Likewise, in the previous studies, our data also confirmed the overlapping expression
338 response of wheat ZIFL genes (Briat et al., 2015). Additionally, under Fe limiting conditions,
339 induction of Zn responsive genes could be an important step towards limiting the non-specific
340 transport activity of transporters which are primarily induced for Fe deficiency. ZIFL are well
341 known for their response towards the presence of excess Zn. During our study, we also observed

342 multiple wheat ZIFLs that responded to excess Zn, either in shoots or roots in a temporal
343 manner. Interestingly, most of the wheat ZIFL genes show the presence of iron responsive cis-
344 element IDE1. IDE1 is one of the primary cis-elements that respond to Fe limiting conditions
345 (Kobayashi et al., 2007). Therefore, we studied the expression of wheat ZIFLs under –Fe
346 condition. Multiple ZIFLs showed specific response towards Fe deficiency, suggesting that iron
347 deficiency response by ZIFLs could be mediated by certain transcription factors like IDE1 that
348 are highly specific for Fe homeostasis. Expression of the few of the ZIFLs like *TaZIFL1.1*,
349 *TaZIFL1.2*, *TaZIFL4.2* and *TaZIFL6.2* were also affected by both Fe and Zn. These results
350 suggest that few of these ZIFLs might be involved in the overlapping pathways of Fe and Zn
351 homeostasis. Such partial overlaps of Zn and Fe homeostasis was reported earlier and is also
352 evident from our work. This may also lead to a speculation for the sharing of a common network
353 of transcription factors related to Fe and Zn interactions. In our study, the promoters of
354 *TaZIFL1.2* and *TaZIFL2.3* showed the presence of IRO2 binding domains that has been
355 previously speculated to be the link between Fe and Zn homeostasis (Ricachenevsky et al.,
356 2011). Nonetheless, only *TaZIFL1.2* respond to –Fe and +Zn stress that is restricted only to
357 shoots. Previously, it was also shown that expression of Arabidopsis ZIF1 remained unaffected
358 in the presence of sub-inhibitory levels of Cd or Cu (Haydon and Cobbette, 2007). Based on the
359 expression response of ZIFL genes during in the presence of heavy metals it seems that *TaZIFL5*
360 and *TaZIFL6.2* could be one of the best candidate genes for the further studies, as both the genes
361 remained unaffected. Nevertheless, careful selection of candidate gene must be done to minimize
362 the cotransport of other undesired metals during micronutrient uptake.

363 In addition to their anticipated role in Fe and Zn homeostasis, their role in root
364 development has been also proven. Plant ZIFL transporters have been reported to regulate

365 stomatal movements by means of polar auxin transport, thereby modulating potassium and
366 proton fluxes in *Arabidopsis* (Remy et al., 2013). Analysis of the expVIP data suggested high
367 expression of wheat ZIFLs (TaZIFL7.1-4A and 4D) under drought condition. Earlier, *zifl-1* and
368 *zifl-2* mutants of *Arabidopsis* showed hypersensitivity to drought stress by disruption of guard
369 cells activity (Remy et al., 2015). *TaZIFL1.2* is the wheat transporter showing highest expression
370 in leaf and highest homology with *AtZIFL1*, thereby belonging to the same clade in the
371 phylogeny tree. In contrast to the expected function of ZIFL in Fe and Zn homeostasis, a putative
372 role has been demonstrated in plant defense. Maize ZIFL referred as *Zm-mfs1* was high induced
373 during plant defense and has been implicated its role for export of antimicrobial compounds
374 during its interaction with the bacterial pathogen (Simmons et al., 2003). In our study, a strong
375 expression of multiple *ZIFL* genes was observed when infected with multiple pathogens
376 suggesting its important role in providing resistance against fungal pathogens (Figure S3).

377 This study concludes that ZIFL transporters are the important players during the crosstalk
378 of Fe and Zn homeostasis. With the recent evidences regarding its role as a potential transporter
379 for nicotinamine and mugineic acids in roots, ZIFL are certainly a priority candidate for uptake
380 and remobilization of micronutrients in the cereal grains like wheat.

381

382 **Conclusion**

383 This is the first comprehensive study that resulted in identification of fifteen putative ZIFL genes
384 from hexaploidy wheat at the homoeolog level. These are the highest number of ZIFL genes
385 reported in plant system till date. Wheat ZIFL were characterized for their expression response in
386 seedlings exposed to excess Zn and Fe starvation. The contrasting expression of these ZIFL in
387 presence of heavy metals suggested their functional redundancy and pinpoint importance of a

388 few for further functional validation. Overall, we identified few candidate ZIFL from hexaploid
389 wheat that could be the important target to address new means to enhance micronutrient uptake.

390

391 **Abbreviations used**

392 CCC1: Ca²⁺-sensitive cross completer 1; YSL: yellow-stripe like protein; ZIFL: Zinc-
393 induced facilitator-1 like gene; CDD: conserved domain database; MFS: Major facilitator
394 superfamily; TM: trans-membrane; HMRE: heavy metal responsive element; IRO2: iron related
395 transcription factor 2; IDEF: iron-deficiency responsive element binding factor 1; QRT-PCR:
396 quantitative real time polymerase chain reaction; TOM: transporter of mugineic acid; TPM:
397 transcript per millions; PM: plasma-membrane

398

399 **Methods**

400 **Identification of the MFS-1 family in wheat**

401 To identify the potential members of *ZIFLs* from MFS_1 transporter family in wheat genome,
402 we used two independent approaches. In the first approach, the Pfam number (PF07690) for
403 MFS_1 was used and sequences were extracted from wheat using the Ensembl wheat database.
404 As a complementary approach, known sequences of *ZiaFL* genes from *A. thaliana*, *O. sativa* and
405 *B. distachyon* were retrieved and used for BLAST analysis against the wheat databases:
406 Ensemble (http://plants.ensemble.org/Triticum_aestivum/) to retrieve the sequences. The
407 identified *MFS_1* superfamily was validated through the domain search in CDD-NCBI database
408 (<https://www.ncbi.nlm.nih.gov/Structure/cdd/wrpsb.cgi>) [33].

409

410 **Identification, classification, and chromosomal distribution of wheat ZIFL genes**

411 To identify putative *TaZIFLs* genes among MFS_1 superfamily sequence, phylogenetic tree was
412 constructed with known ZIFLs from different plants that separated the ZIFL cluster from the rest
413 of the MFS_1 superfamily members. This distribution of genes in ZIFL cluster was validated
414 through the presence of ZIFL specific signature sequences. To construct the phylogenetic tree
415 one hundred seventy-nine wheat MFS_1 superfamily protein sequence was retrieved from Pfam
416 no. (PF07690). In addition to that, thirteen-protein sequence of ZIFL from *O. sativa*, five from
417 *Zea mays* and three from *Arabidopsis* were used. Identified TaZIFL genes were named according
418 to their corresponding rice orthologs having maximum number of ZIFL reported. The name
419 indicates corresponding ortholog from rice followed by chromosomal and genomic location e.g.
420 *TaZIFL3-4A*, *TaZIFL3-4B* and *TaZIFL3-4D* represent three homoeologous of *TaZIFL* gene in
421 chromosome four of all the three A, B and D sub-genomes and it is an ortholog of *OsZIFL3*.
422 Phylogenetic analysis was also done with identified ZIFL proteins of wheat and other plant
423 species (*O. sativa*, *Z. mays* and *Arabidopsis*) to know the evolutionary relationship among them.
424 All the proteins were aligned through MUSCLE algorithm and a rooted phylogenetic tree was
425 used to construct with the Neighbor-joining (NJ) method using MEGA7 software with 1000
426 bootstrap replicates [34]. To determine the distribution of ZIFL genes in the wheat
427 chromosomes, the position for each ZIFL genes was obtained using wheat Ensembl database
428 (ftp://ftp.ensemblgenomes.org/pub/plants/release-34/fasta/triticum_aestivum).

429

430 **Analysis of conserved domains, gene arrangements and subcellular localization of wheat** 431 **ZIFL**

432 The divergence and conservation of motifs in wheat ZIFL proteins were also identified by using
433 MEME (Multiple Expectation Maximization for Motif Elicitation) program version 5.0.2

434 (<http://meme-suite.org>) [35] with maximum motif width, 50; maximum number of motifs,15; and
435 minimum motifs width. Gene Structure Display Server (GSDS 2.0) was used to analyze the gene
436 structure. Individual wheat ZIFL's CDS and corresponding genomic DNA were aligned to
437 identify the intron-exon arrangement. Using ExPasy Compute PI/MW online tool
438 (<http://us.expasy.org/tools/protparam.html>) the predicted isoelectric points and molecular
439 weights of putative TaZIFLs were calculated. To predict terminal ends and number of
440 transmembrane domains, TMHMM (<http://www.cbs.dtu.dk/services/TMHMM/>) was utilized.
441 The putative protein sequences of ZIFL genes were further *in silico* analyzed predict their
442 subcellular localization by WoLF PSORT (<https://wolfpsort.hgc.jp/>) prediction program [36].
443

444 **Plant material and Fe, Zn and heavy metals treatments**

445 For giving various zinc and iron treatment (+Zn) and (-Fe), seeds of *Triticum aestivum* cv. C306
446 was used. The seeds were washed with double autoclaved water for the removal of dirt followed
447 by surface sterilization with 1.2% Sodium hypochlorite prepared in 10% ethanol. Seeds were
448 stratified by keeping them overnight at 4 °C on moist Whatman filter papers in a Petri dish. The
449 stratified seeds were further allowed to germinate at room temperature. Healthy seedlings were
450 transferred to phytaboxes (12-15 seedlings/phytabox) and grown in autoclaved water in growth
451 chamber for 5 days. Five days old plantlets were subjected to different Zn and Fe conditions and
452 grown in Hoagland media [37] supplemented with either 2.5 µM of Fe (III) EDTA for iron
453 deficient condition (-Fe) or 200µM of ZnSO₄.7H₂O for zinc surplus experiment (+Zn). Seedlings
454 grown in the Hoagland media containing 20 µM of Fe (III) EDTA and 2 µM of ZnSO₄.7H₂O
455 were used for control experiments. The plantlets (5 days post germination) tissues were collected
456 after 3 and 6 days (D) post treatments along with the respective controls. Every alternate day, the

457 seedlings in the phyta-boxes were supplemented with the fresh media. For heavy metal treatment
458 the 5 days old plantlets were subjected to cadmium (50 μ M CdCl₂), Cobalt (50 μ M CoCl₂),
459 Nickel (50 μ M NiCl₂) treatment. The tissue sample (root and shoot) were collected after 15 days
460 of treatment. (These experiments were repeated twice, frozen in liquid nitrogen and store at -
461 80°C.

462

463 **RNA isolation, cDNA preparation and qRT-PCR analysis**

464 Total RNA was extracted from harvested roots and shoot samples using TRIZOL RNA
465 extraction method. Turbo DNafree kit (Invitrogen) was used to remove the genomic DNA. RNA
466 samples were then quantified on nanodrop and subsequently, 2 μ g of total RNA was used to
467 prepare cDNA by using SuperScript III First-Strand Synthesis System (Invitrogen). For
468 expression analysis qRT-PCR primers were designed from the conserved region of respective
469 *TaZIFL* genes. (Table S7). Amplicons arising from these primers were also processed for
470 sequencing to avoid any cross amplifications of the *ZIFL* genes. 10X diluted cDNA and SYBER
471 Green I (QuantiFast[®] SYBR[®] Green PCR Kit, Qiagen) was used to perform qRT-PCR on 7500
472 Fast Real-Time PCR System (Applied Biosystems, USA). The relative mRNA abundance was
473 normalized with wheat *ARF* (*ADP-Ribosylation Factor*, AB050957.1; [38, 39]. The relative
474 expression was calculated through delta-delta CT-method ($2^{-\Delta\Delta CT}$) [40]. The statistical
475 significance of expression data was determined using student's t-test (p-value <0.05).

476

477 ***In-silico* expression analysis**

478 For *In-silico* expression analysis 35 *TaZIFL* genes were selected and wheat expression browser,
479 expVIP [<http://www.wheat-expression.com/>] was used to extract the expression values in the

480 form of TPMs. These values were then used to build heatmaps using MeV software
481 [<http://mev.tm4.org/>]. While absolute values were used for development and tissue-specific data,
482 fold change values were used for stress conditions where a gene was taken to be upregulated if
483 fold change was greater than 2 and downregulated if less than 0.66. For abiotic stress,
484 expression for two studies, phosphate starvation [41] and heat, drought and heat-drought stress
485 [42] was studied. In case of biotic stress, the studies considered were [43–45].

486

487 **References**

- 488 1. Nyaradi A, Li J, Hickling S, Foster J, Oddy WH. The role of nutrition in children ' s
489 neurocognitive development , from pregnancy through childhood. *Front Hum Neurosci.*
490 2013;7:1–16.
- 491 2. Gibson RS. The Rank Prize Lecture Zinc□: the missing link in combating micronutrient
492 malnutrition in developing countries. *Proc Nutr Soc.* 2006;65:51–60.
- 493 3. Wishart K. Vitamins & Minerals Increased Micronutrient Requirements during
494 Physiologically Demanding Situations□: Review of the Current Evidence. *Vitam Miner.* 2017;6.
- 495 4. Rout, G.R.; Sahoo S. ROLE OF IRON IN PLANT GROWTH AND. *Rev Agric Sci.*
496 2015;100:1726–37.
- 497 5. Hafeez B, Khanif YM, Saleem M. Role of Zinc in Plant Nutrition- A Review. *Am J Exp*
498 *Agric.* 2013;3:374–91.
- 499 6. Kawachi M, Kobae Y, Mori H, Tomioka R, Lee Y, Maeshima M. A Mutant Strain
500 *Arabidopsis thaliana* that Lacks Vacuolar Membrane Zinc Transporter MTP1 Revealed the
501 Latent Tolerance to Excessive Zinc. *Plant Cell Physiol.* 2018;50:1156–70.

- 502 7. Stein RJ. Plant Science Differential regulation of the two rice ferritin genes (OsFER1 and
503 OsFER2). Plant Sci. 2009;177:563–9.
- 504 8. Eide D, Broderius M, Fett J, Guerinot M Lou, Fettu J, Lou M. A novel iron-regulated metal
505 transporter from plants identified by functional expression in yeast. Proc Natl Acad Sci.
506 2014;93:5624–8.
- 507 9. Lee S, An G. Over-expression of OsIRT1 leads to increased iron and zinc accumulations in
508 rice. plant cell Environ. 2009;32:408–16.
- 509 10. Morrissey J, Guerinot M Lou. Iron Uptake and Transport in Plants: The Good, the Bad, and
510 the Ionome. Chem Rev. 2009;109:4553–67. doi:10.1021/cr900112r.
- 511 11. Morel M, Crouzet J, Gravot A, Auroy P, Leonhardt N, Vavasseur A RP. AtHMA3 , a P 1B -
512 ATPase Allowing Cd / Zn / Co / Pb Vacuolar Storage in Arabidopsis 1 [W]. Plant Physiol.
513 2009;149:894–904.
- 514 12. Yoneyama T, Ishikawa S, Fujimaki S. Route and Regulation of Zinc , Cadmium , and Iron
515 Transport in Rice Plants (*Oryza sativa* L .) during Vegetative Growth and Grain Filling□: Metal
516 Transporters , Metal Speciation , Grain Cd Reduction and Zn and Fe Biofortification. Int J Mol
517 Sci. 2015;16:19111–29.
- 518 13. Ishimaru Y, Bashir K. Zn Uptake and Translocation in Rice Plants. Rice. 2011;4:21–7.
- 519 14. Römheld V, Schaaf G. Soil Science and Plant Nutrition Iron transport in plants□: Future
520 research in view of a plant nutritionist and a molecular biologist Iron Transport in Plants□:
521 Future Research in View of a Plant. Soil Sci Plant Nutr. 2011;50:1002–12.
- 522 15. Sinclair SA, Kraemer U. The Zinc homeostasis network of land plants. Biochim Biophys
523 Acta. 2012;1823.

- 524 16. Kumar A, Kaur G, Goel P, Bhati KK, Kaur M, Shukla V. Genome-wide analysis of
525 oligopeptide transporters and detailed characterization of yellow stripe transporter genes in
526 hexaploid wheat. *Funct Integr Genomics*. 2018;19:75–90.
- 527 17. Haydon MJ, Cobbett CS. A Novel Major Facilitator Superfamily Protein at the Tonoplast
528 Influences Zinc Tolerance and Accumulation. *Plant Physiol*. 2007;143:1705–19.
- 529 18. Ricachenevsky FK, Sperotto RA, Menguer PK, Sperb ER, Lopes KL, Fett JP. ZINC-
530 INDUCED FACILITATOR-LIKE family in plants□: lineage-specific expansion in
531 monocotyledons and conserved genomic and expression features among rice (*Oryza sativa*)
532 paralogs. *BMC Plant Biol*. 2011;11:20. doi:10.1186/1471-2229-11-20.
- 533 19. Haydon MJ, Kawachi M, Wirtz M, Hillmer S, Kra U. Vacuolar Nicotianamine Has Critical
534 and Distinct Roles under Iron Deficiency and for Zinc Sequestration in Arabidopsis. *Plant Cell*.
535 2012;24:724–37.
- 536 20. Nozoye T, Nagasaka, S.; Kobayashi, T.;Takahashi, M.;Sato, Y.; Sato, Y.; Uozumi, N.;
537 Nakanishi, H.; Nishizawa NK. Phytosiderophore Efflux Transporters Are Crucial for Iron
538 Acquisition in Gramineous Plants * □. *J Biol Chem*. 2011;286:5446–54.
- 539 21. Nozoye T, Nagasaka S, Kobayashi T, Sato Y, Uozumi N, Nakanishi H, et al. The
540 Phytosiderophore Efflux Transporter TOM2 Is Involved in Metal Transport in Rice. *J Biol*
541 *Chem*. 2015;290:27688–99. doi:10.1074/jbc.M114.635193.
- 542 22. Remy, E.; Cabrito, T. R.; Baster P.; Batista, R.A.; Teixeira, M. C.; Friml, J.; Sa-Correia, I.;
543 Duque P. A Major Facilitator Superfamily Transporter Plays a Dual Role in Polar Auxin
544 Transport and Drought Stress Tolerance in Arabidopsis. *Plant Cell*. 2013;25:901–26.

- 545 23. Simmons CR, Fridlender M, Navarro PA, Yalpani N. A maize defense-inducible gene is a
546 major facilitator superfamily member related to bacterial multidrug resistance efflux antiporters.
547 *Plant Mol Biol.* 2003;52:433–46.
- 548 24. Connorton JM, Jones ER, Rodríguez-ramiro I, Fairweather-tait S. Wheat Vacuolar Iron
549 Transporter TaVIT2 Transports Fe and Mn and Is Effective for Biofortification 1 [OPEN].
550 *Plant Physiol.* 2017;174:2434–44.
- 551 25. Singh, S.P.; Keller, B.; Gruissem, W.; Bhullar NK. Rice NICOTIANAMINE SYNTHASE 2
552 expression improves dietary iron and zinc levels in wheat. *Theor Appl Genet.* 2017;130:283–92.
- 553 26. Aggarwal S, Kumar A, Bhati KK, Kaur G, Shukla V, Tiwari S, et al. RNAi-Mediated
554 Downregulation of Inositol Pentakisphosphate Kinase (IPK1) in Wheat Grains Decreases Phytic
555 Acid Levels and Increases Fe and Zn Accumulation. *Front Plant Sci.* 2018;9:1–12.
556 doi:10.3389/fpls.2018.00259.
- 557 27. Gillies SA, Futardo A, Henry RJ. Gene expression in the developing aleurone and starchy
558 endosperm of wheat. 2012;10:668–79.
- 559 28. Pearce S, Tabbita F, Cantu D, Buffalo V, Avni R, Vazquez-gross H, et al. Regulation of Zn
560 and Fe transporters by the GPC1 gene during early wheat monocarpic senescence. *BMC Plant*
561 *Biol.* 2014;14:1–23.
- 562 29. Feigl, G., Lehotai, N.; Molnar, A.; Ordog, A.; Rodriguez-Ruiz, M.; Palma, J. M.; Corpas, . J.;
563 Erdei L.; Kolbert Z. Zinc induces distinct changes in the metabolism of reactive oxygen and
564 nitrogen species (ROS and RNS) in the roots of two Brassica species with different sensitivity
565 to zinc stress. *Ann Bot.* 2015;116:613–25.

- 566 30. Briat J, Rouached H, Tissot N, Gaymard F, Dubos C. Integration of P , S , Fe , and Zn
567 nutrition signals in *Arabidopsis thaliana*: potential involvement of PHOSPHATE
568 STARVATION. *Front Plant Sci.* 2015;6:1–16.
- 569 31. Kobayashi T, Ogo Y, Itai RN, Nakanishi H, Takahashi M, Mori S, et al. The transcription
570 factor IDEF1 regulates the response to and tolerance of iron deficiency in plants. *Proc Natl Acad*
571 *Sci.* 2007;104:19150–5. doi:10.1073/pnas.0707010104.
- 572 32. Remy E, Cabrito R, Batista RA, Teixeira MC, Sa I, Duque P. The Major Facilitator
573 Superfamily Transporter ZIFL2 Modulates Cesium and Potassium Homeostasis in *Arabidopsis*.
574 *Plant Cell Physiol.* 2015;56:148–62.
- 575 33. Marchler-bauer A, Lu S, Anderson JB, Chitsaz F, Derbyshire MK, Deweese-scott C, et al.
576 CDD: a Conserved Domain Database for the functional annotation of proteins. *Nucleic Acids*
577 *Res.* 2011;39:225–9.
- 578 34. Kumar, S.; Nei, M.; Dudley, J.; Tamura K. NIH Public Access. *Br Bioinforma.* 2009;9:299–
579 306.
- 580 35. Bailey TL, Boden M, Buske FA, Frith M, Grant CE, Clementi L, et al. MEME S UITE:
581 tools for motif discovery and searching. *Nucleic Acids Res.* 2009;37:1–7.
- 582 36. Horton P, Park K, Obayashi T, Fujita N, Harada H, Nakai K. WoLF PSORT: protein
583 localization predictor. *Nucleic Acids Res.* 2007;35:585–7.
- 584 37. Hoagland. *The Water-Culture Method for Growing Plants without Soil THE COLLEGE OF*
585 *AGRICULTURE.* 1950.
- 586 38. Bhati KK, Aggarwal S, Sharma S, Mantri S, Singh SP, Bhalla S, et al. *Plant Science*
587 *Differential expression of structural genes for the late phase of phytic acid biosynthesis in*

- 588 developing seeds of wheat (*Triticum aestivum* L .). *Plant Sci.* 2014;224:74–85.
589 doi:10.1016/j.plantsci.2014.04.009.
- 590 39. Shukla V, Kaur M, Sipla A, Bhati KK, Kaur J. Tissue specific transcript profiling of wheat
591 phosphate transporter genes and its association with phosphate allocation in grains. *Sci Rep.*
592 2016;6:1–12.
- 593 40. Livak KJ, Schmittgen TD. Analysis of Relative Gene Expression Data Using Real- Time
594 Quantitative PCR and the 2^{-ΔΔC_T} Method. *Methods.* 2001;408:402–8.
- 595 41. Oono Y, Kobayashi F, Kawahara Y, Yazawa T, Handa H, Itoh T. Characterisation of the
596 wheat (*triticum aestivum* L .) transcriptome by de novo assembly for the discovery of
597 phosphate starvation-responsive genes: gene expression in Pi-stressed wheat. *BMC Genomics.*
598 2013;14:1. doi:10.1186/1471-2164-14-77.
- 599 42. Liu Z, Xin M, Qin J, Peng H, Ni Z, Yao Y, et al. Temporal transcriptome profiling reveals
600 expression partitioning of homeologous genes contributing to heat and drought acclimation in
601 wheat (*Triticum aestivum* L.). *BMC Plant Biol.* 2015;15:152. doi:10.1186/s12870-015-0511-8.
- 602 43. Kugler KG, Siegwart G, Nussbaumer T, Ametz C, Spannagl M, Steiner B, et al. Quantitative
603 trait loci-dependent analysis of a gene co-expression network associated with *Fusarium* head
604 blight resistance in bread wheat (*Triticum aestivum* L .). *BMC Genomics.* 2013;14:728.
- 605 44. Yang F, Li W, Jørgensen HJL. Transcriptional Reprogramming of Wheat and the
606 Hemibiotrophic Pathogen *Septoria tritici* during Two Phases of the Compatible Interaction. *PLoS*
607 *One.* 2013;8:1–15.

608 45. Zhang L, Zhang L, Xia C, Zhao G, Jia J, Kong X. The Novel Wheat Transcription Factor
609 TaNAC47 Enhances Multiple Abiotic Stress Tolerances in Transgenic Plants. *Front Plant Sci.*
610 2016;6:1–12.

611 **Declarations**

612 **Ethics approval and consent to participate**

613 Not applicable

614 **Consent to publish**

615 Not applicable

616 **Availability of data and materials**

617 Not applicable

618 **Competing interests**

619 The authors declare that they have no competing interests

620 **Funding**

621 This research was funded by the NABI-CORE grant to AKP

622

623 **Acknowledgments**

624 The authors thank Executive Director, NABI for facilities and support. This research was funded
625 by the NABI-CORE grant to AKP. Thanks to the International Wheat Genome Sequencing
626 Consortium for providing the high-quality wheat genome resources.

627 **Author contribution**

628 AKP and SS conceptualized and planned the work. SS, AK, JK and AKP designed the study. SS
629 and AK performed all the experiments. GK and SS performed the Bioinformatics work. SS, AK
630 and AKP analyzed the data. AKP, GK, JK and SS wrote the manuscript. All the authors
631 reviewed and edited the final version of the manuscript.

632

633 **Legends for the Figures:**

634 **Figure 1.** Phylogenetic analysis of wheat ZIFL protein sequences. The analysis was performed
635 by using thirty-five ZIFL protein sequences from wheat, thirteen from *Oryza sativa*, seven from
636 *Zea mays* and three from *Arabidopsis*. Rooted phylogenetic tree was constructed by using
637 Neighbour-joining method using MEGA7 software with 1000 bootstrap replicates.

638 **Figure 2.** Genomic and chromosomal distribution of wheat ZIFLs on wheat genome.
639 Distribution of thirty-five TaZIFLs across: **a.** A, B and D sub genomes. **b.** Wheat chromosomal
640 distribution. **c.** Chromosomal distribution share on different Chromosome and genome.

641 **Figure 3.** Intron exon arrangement and protein conservation. The intron-exon structure was
642 obtained using Gene Structure Display Server (GSDS 2.0:) Yellow boxes and black lines depict
643 the introns and exons, respectively.

644 **Figure 4.** Protein sequence analysis for conserved and unique motifs in wheat ZIFL. **a.**
645 Conserved motifs across 15 TaZIFL proteins, as obtained from MEME. Different colors
646 represent distinct motifs. **b.** Unique motifs found through MEME for group 2, group 4, as well as
647 TaZIFL6.2.

648 **Figure 5.** Relative gene expression levels of wheat ZIFLs under +Zn condition. Gene expression
649 profiles of wheat ZIFL genes were studied in a) roots and b) shoots. Total RNA was extracted
650 from the wheat seedlings subjected to three and six days of treatments +Zn. The roots and shoots
651 samples were collected, and qRT-PCR was performed on the DNA free RNAs. A total of 2 µg of
652 RNA was used for cDNA synthesis. C_t values were normalized against wheat *ARF1* as an
653 internal control. Data represents mean of two biological replicates each treatment containing 15-

654 18 seedlings. Vertical bars represent the standard deviation. # on the bar indicates that the mean
655 is significantly different at $p < 0.05$ with respect to their respective control samples.

656 **Figure 6.** Relative gene expression levels of wheat ZIFLs under –Fe condition. Gene expression
657 profiles of wheat ZIFL genes were studied in a) roots and b) shoots. Total RNA was extracted
658 from the wheat seedlings subjected to three and six days of treatments. The roots and shoots
659 samples were collected, and qRT-PCR was performed on the DNA free RNAs. A 2 μ g of total
660 RNA was used for cDNA synthesis. C_t values were normalized against wheat *ARF1* as an
661 internal control. Data represents mean of two biological replicates with each treatment
662 containing 15-18 seedlings. Vertical bars represent the standard deviation. # on the bar indicates
663 that the mean is significantly different at $p < 0.05$ with respect to their respective control
664 treatments.

665 **Figure 7.** qRT-PCR expression analysis of shoots and roots of wheat seedlings exposed to
666 multiple heavy metals (Ni, Co and cd). Five days old wheat seedlings were exposed to the
667 mentioned heavy metals for the period of 14 days. Total RNA was extracted from the treated and
668 control samples and 2 μ g of RNA was used to construct the cDNA. C_t values were normalized
669 against wheat *ARF1* as an internal control. Fold expression values were calculated relative to the
670 control tissue of the mentioned wheat ZIFL. Vertical bars represent the standard deviation. #
671 represent the significantly difference at $p < 0.05$ with respect to their respective control
672 treatments.

673 **Figure 8.** Heat map for relative expression of putative *TaZIFL* genes in different tissues and at
674 multiple developmental stages. Heatmaps were generated using expression values from expVIP
675 database for grain, leaf, root, spike and shoot tissues. Green to red color change depicts increase
676 in transcript expression, as shown by the color bar.

677

678 **Legends for the Supplementary Figures:**

679 **Figure S1** Neighbor-Joining (NJ) tree for MFS_1 family of proteins from *Oryza sativa*,
680 *Brachypodium distachyon*, *Zea mays* and *Triticum aestivum* constructed using MEGA7.0
681 software with a bootstrap replicate value of 1000. The phylogenetic tree shows ZIFL proteins
682 clustering into a distinct clade within the MFS family.

683 **Figure S2** Showing MEGA alignments for signature sequences specific for ZIFLs, namely,
684 ZIFL MFS signature motif, the anti-porter signature, Cys-containing, His-containing signatures.

685 **Figure S3** Relative expression of putative *TaZIFL* genes under various abiotic and biotic
686 stresses: (A) Heat maps of *TaZIFL* genes generated using fold change values obtained after
687 processing of TPM values from wheat expression database expVIP under various abiotic
688 (Phosphate starvation, Drought, Heat and Drought-Heat) (B) Biotic stresses (*Fusarium* heat
689 blight, *Septoria tritici*, stripe Rust and Powdery mildew). Color bar shows the fold change
690 values, thereby green color represents downregulation, black represents no change and red color
691 represents upregulation.

692

693 **Legend for Supplementary Tables:**

694 **Table S1:** List of 179 wheat sequence IDs extracted for MFS_1 family, Pfam ID: PF07690 using
695 ensembl wheat database

696 **Table S2:** Detailed information for 35 putative wheat ZIFLs identified. Table includes gene IDs,
697 chromosomal locations, CDS and protein lengths, molecular weight and pI for each of the
698 obtained putative *TaZIFLs*.

699 **Table S3:** Conserved motifs identified in putative TaZIFLs using MEME. The consensus
700 sequence logo, e-values and the number of sequences in which each motif was found are listed.

701 **Table S4:** ZIFL Signature motifs (Cys, His, MFS and MFS antiporter) and their locations in all
702 TaZIFLs. The motif positions were mapped to the TM-HMM predicted TaZIFL protein
703 structures to obtain the location of motifs.

704 **Table S5:** Cis-elements of wheat ZIFLs along with their positions in the promoter. HMRE-
705 heavy metal responsive element, IRO2- iron related transcription factor 2, MRE: metal
706 responsive element, IDE1: iron-deficiency responsive element binding factor 1.

707 **Table S6:** Table listing the details and expression values extracted from expVIP for different
708 developmental stages and tissues, as well as fold change values obtained after processing the
709 TPM values for the stress conditions (Abiotic stress: phosphate starvation; heat, drought,
710 combined heat-drought stress, & Biotic stress: Fusarium heat blight, *Septoria tritici*, stripe Rust
711 and Powdery mildew).

712 **Table S7:** List of the primers used during the current study.

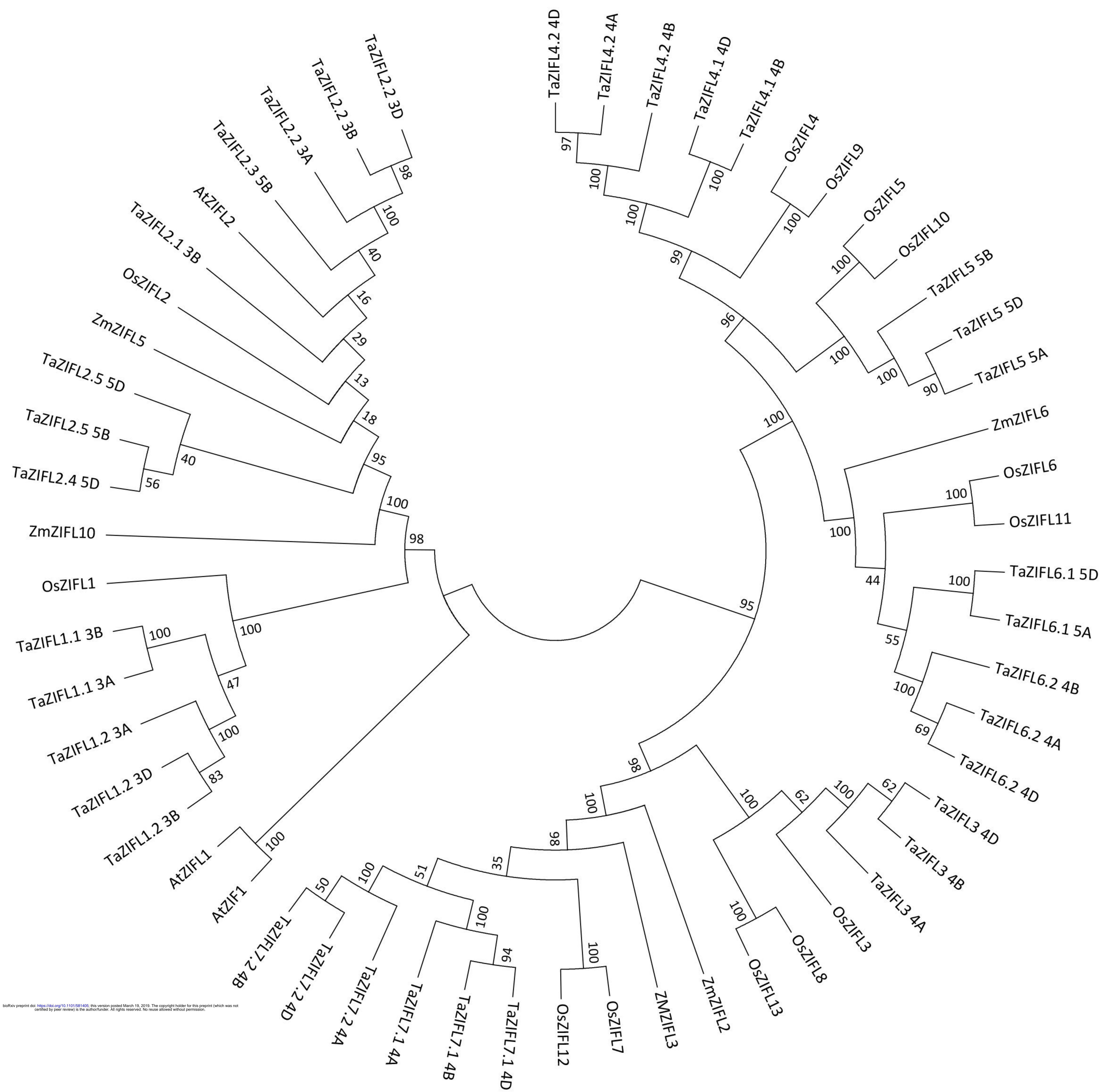
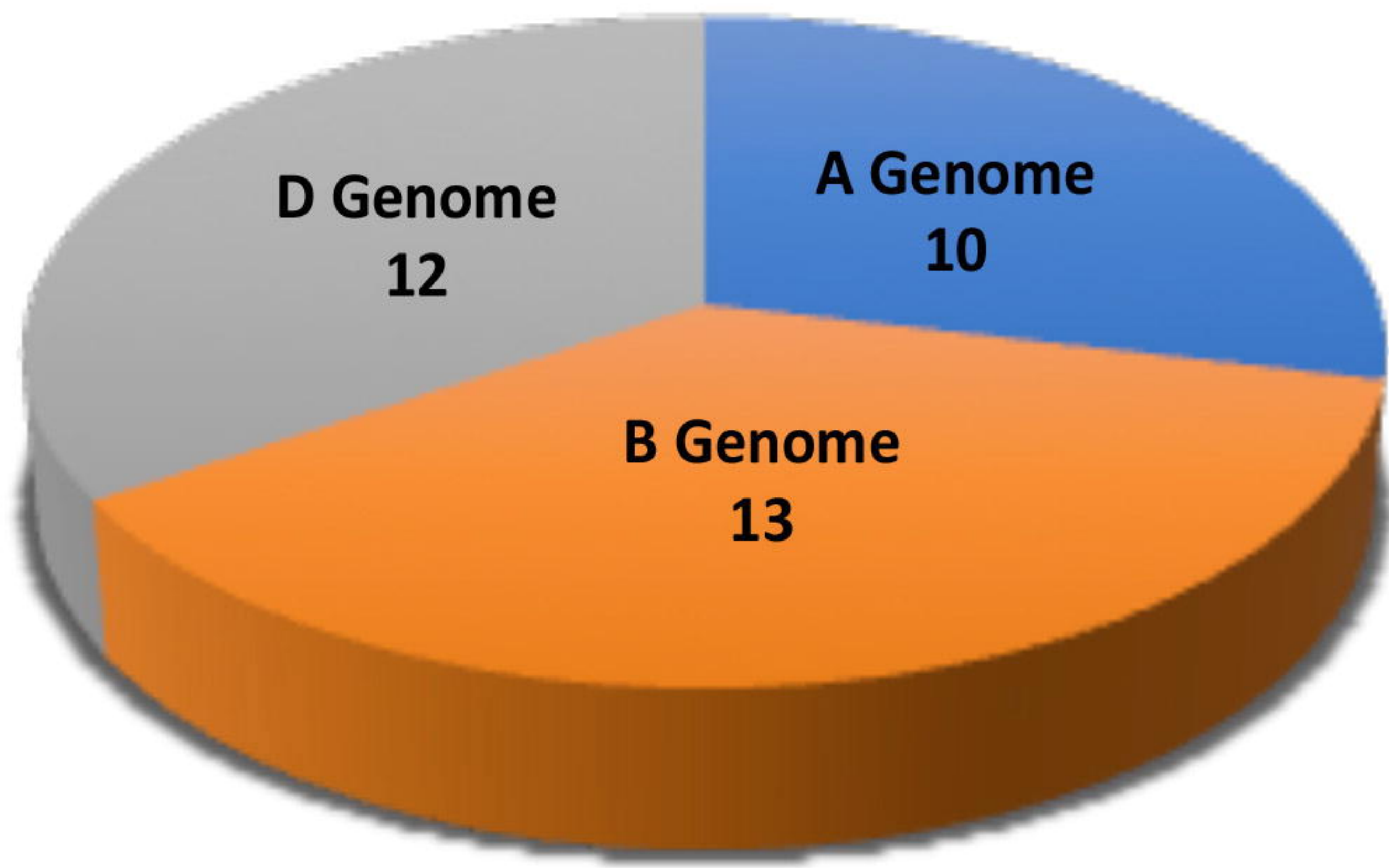
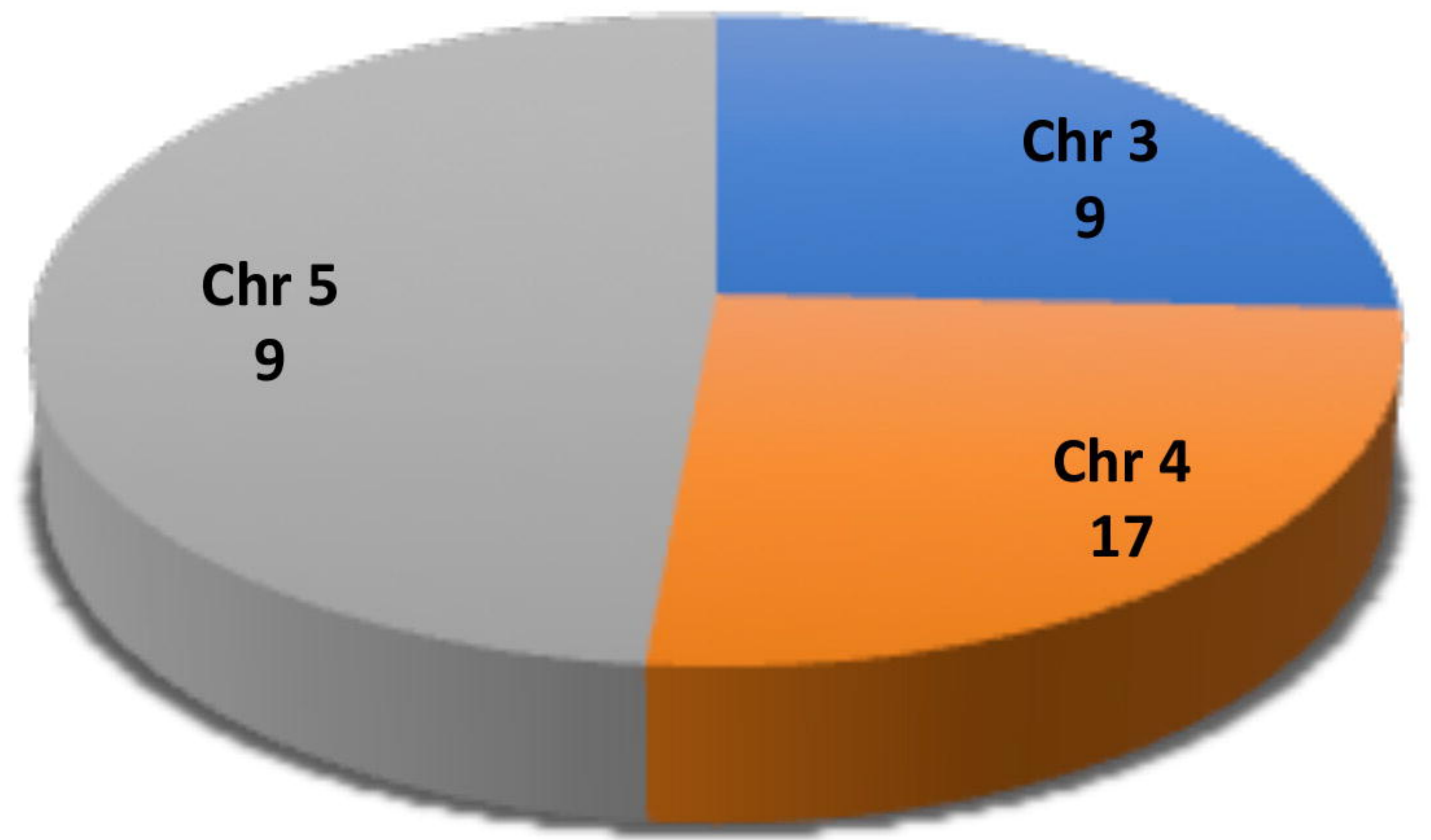


Figure 1

a.



b.



c.

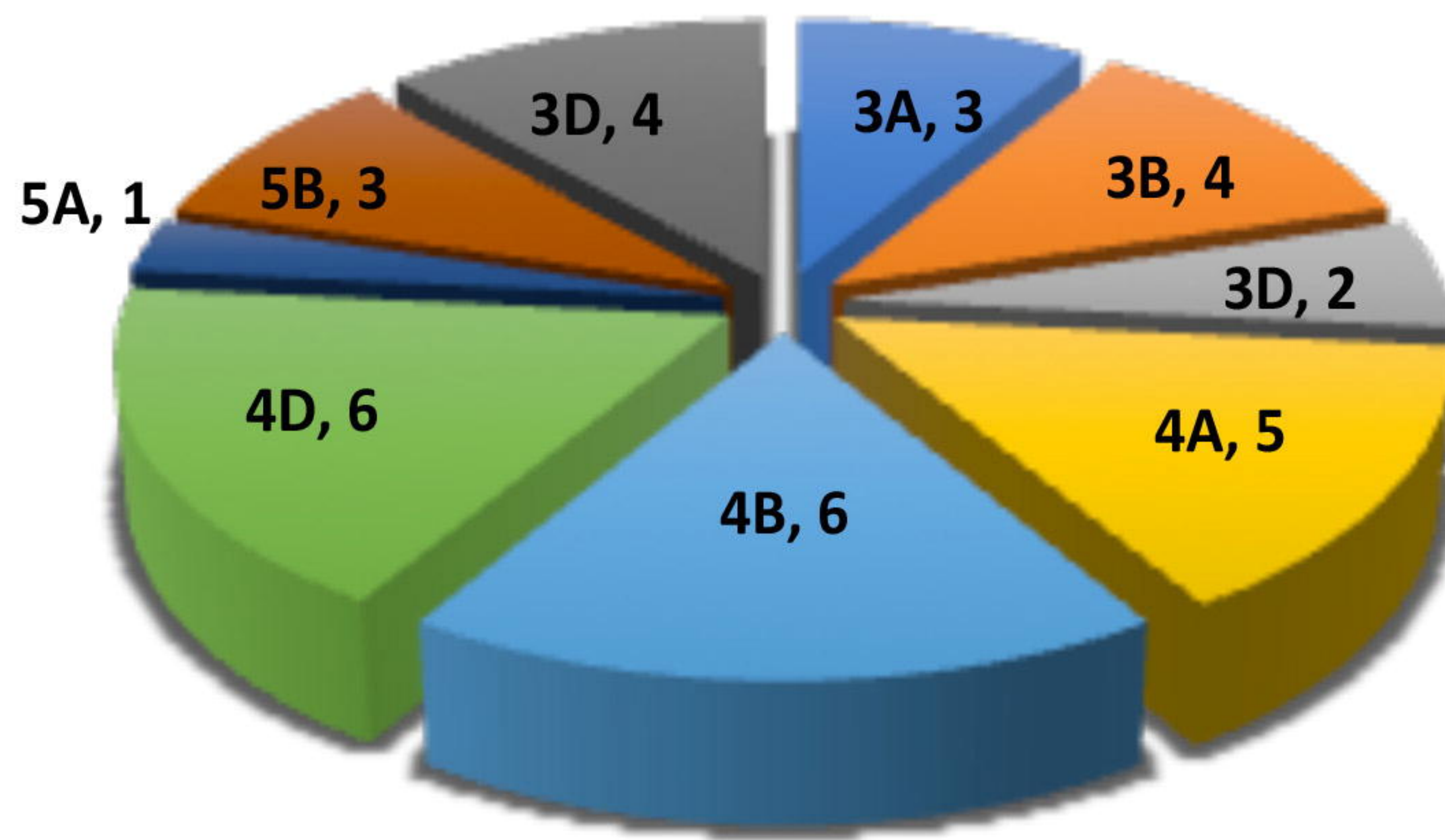


Figure 2

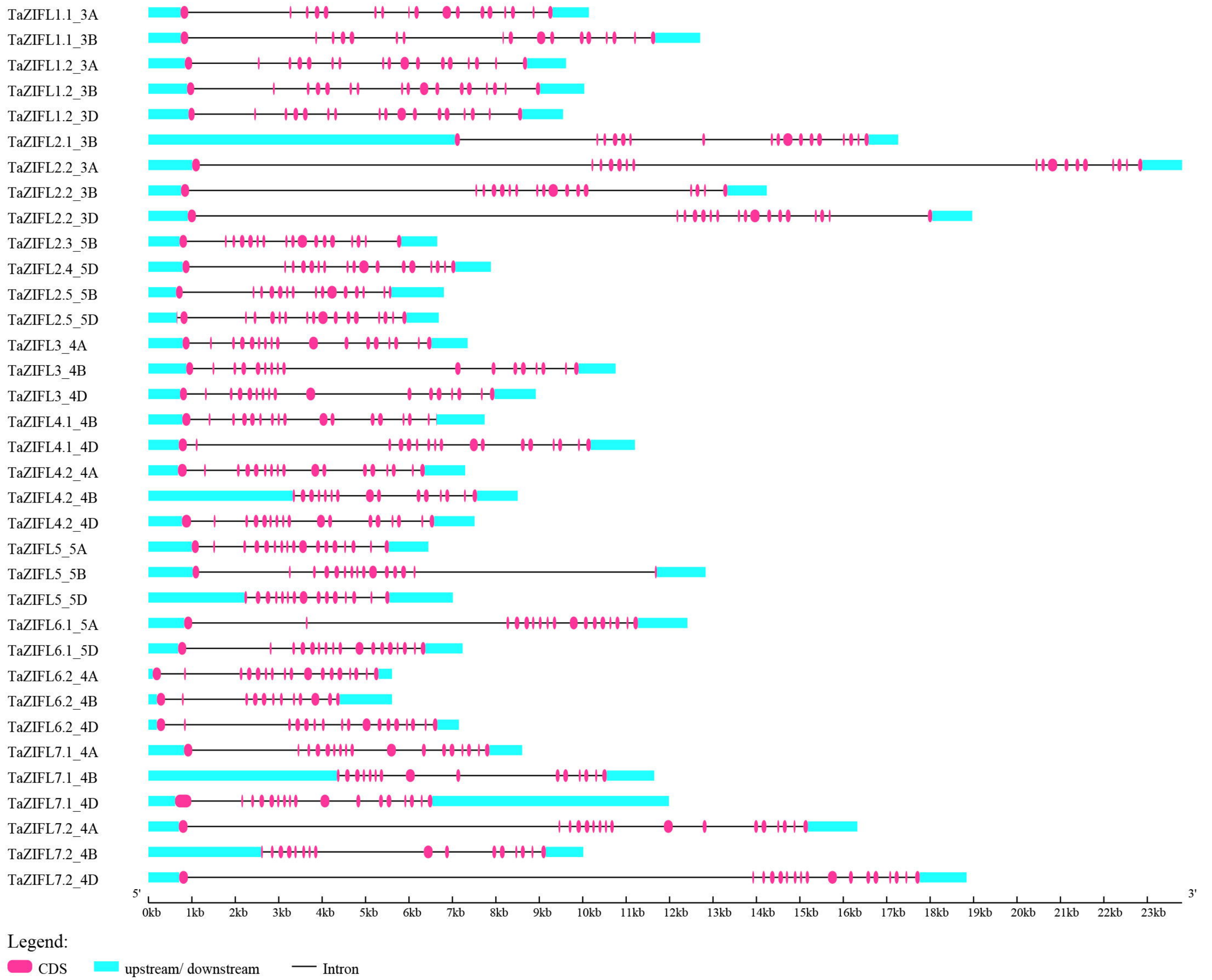
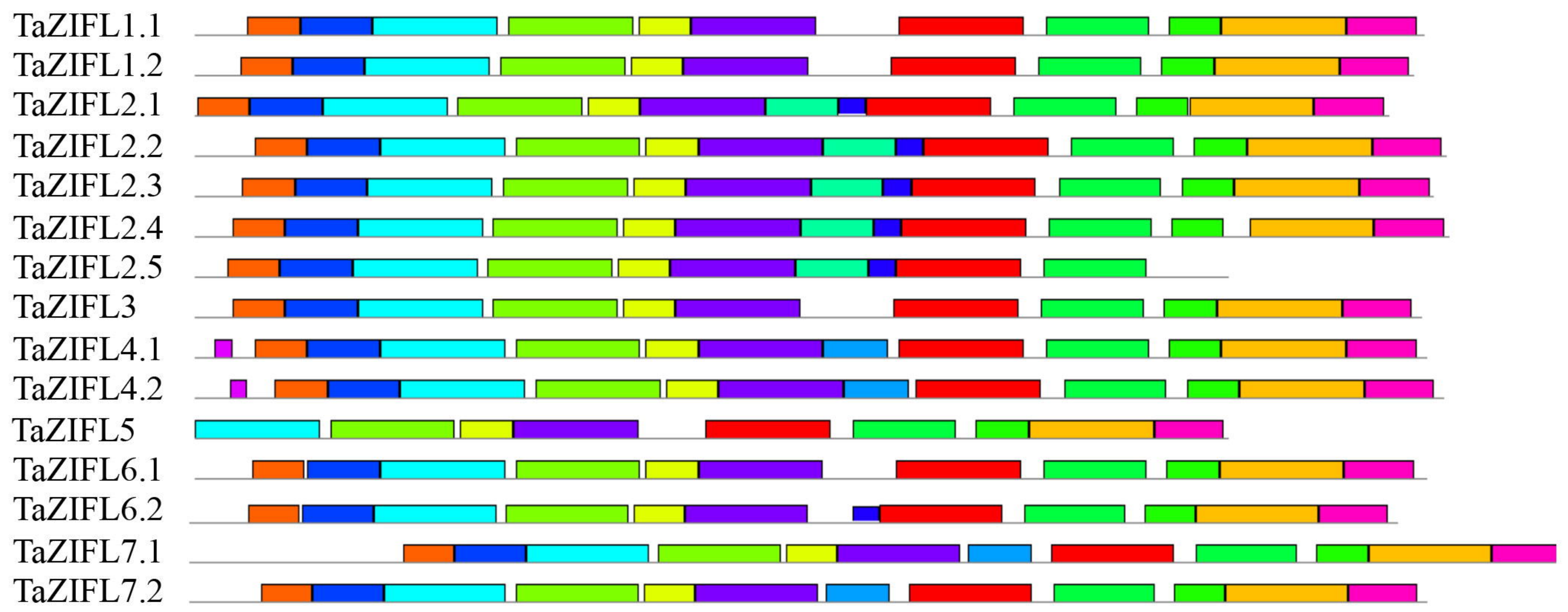


Figure 3

a



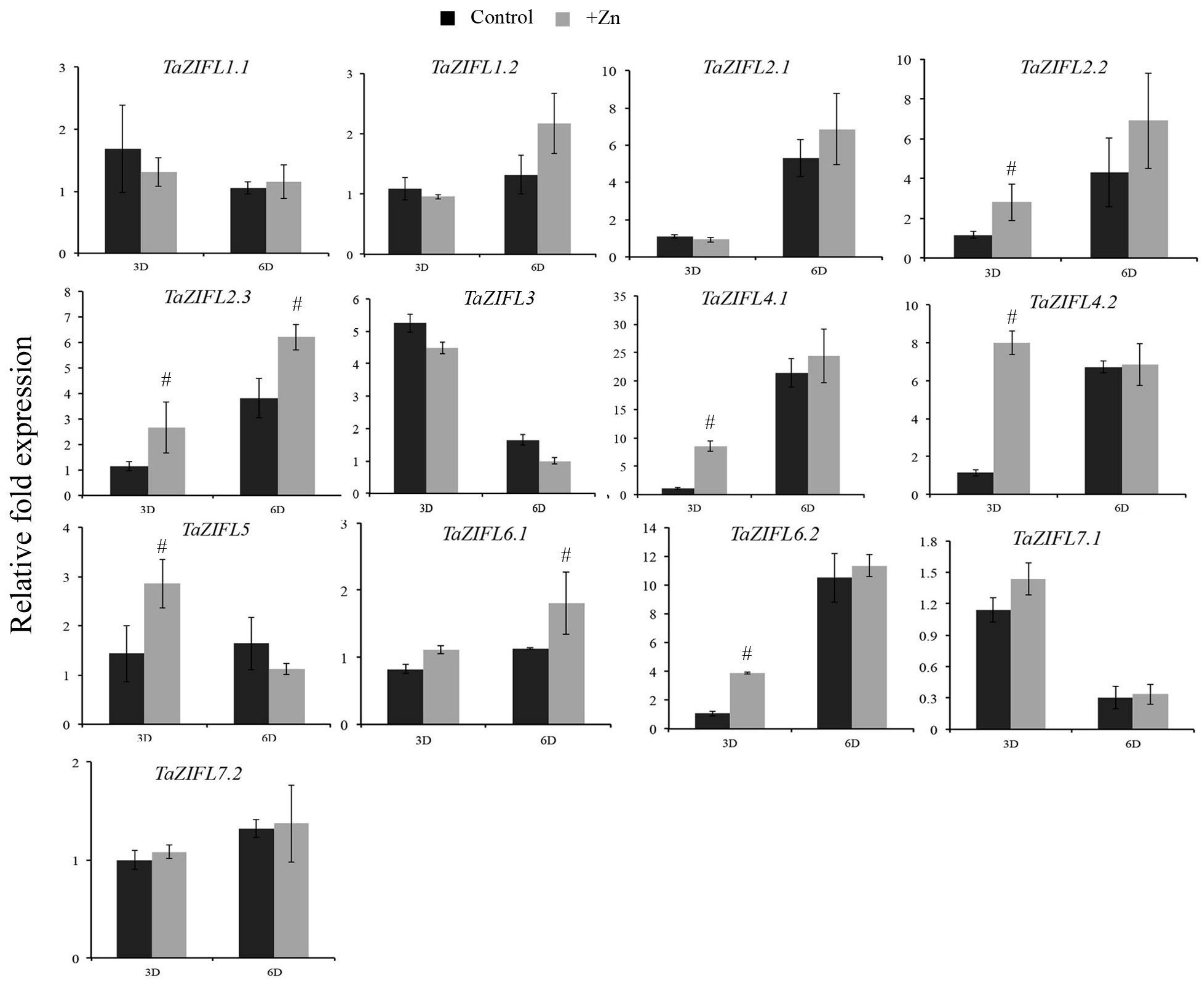
b



bioRxiv preprint doi: <https://doi.org/10.1101/081405>; this version posted March 19, 2019. The copyright holder for this preprint (which was not certified by peer review) is the author/funder. All rights reserved. No reuse allowed without permission.

Figure 4

a



b

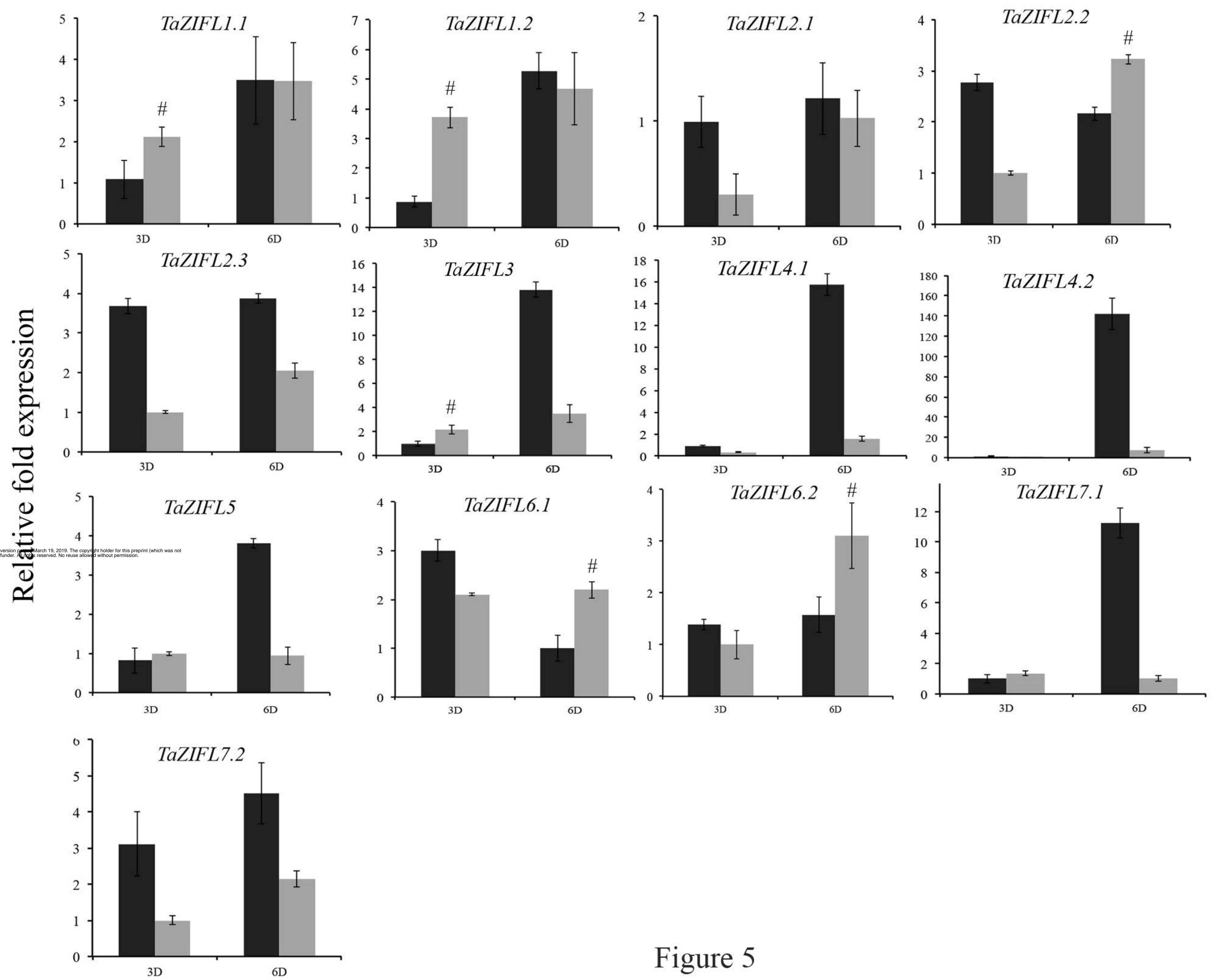
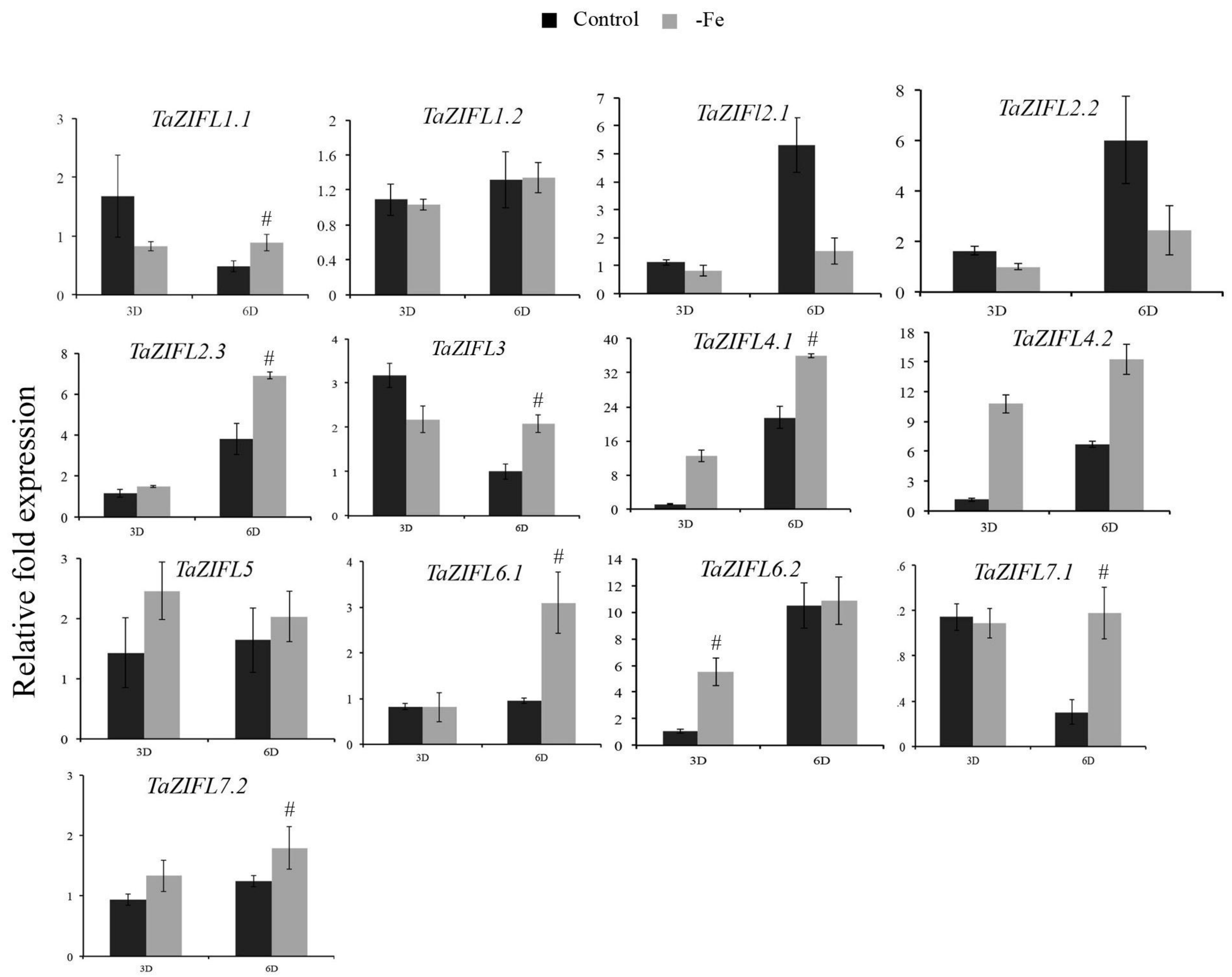


Figure 5

a



b

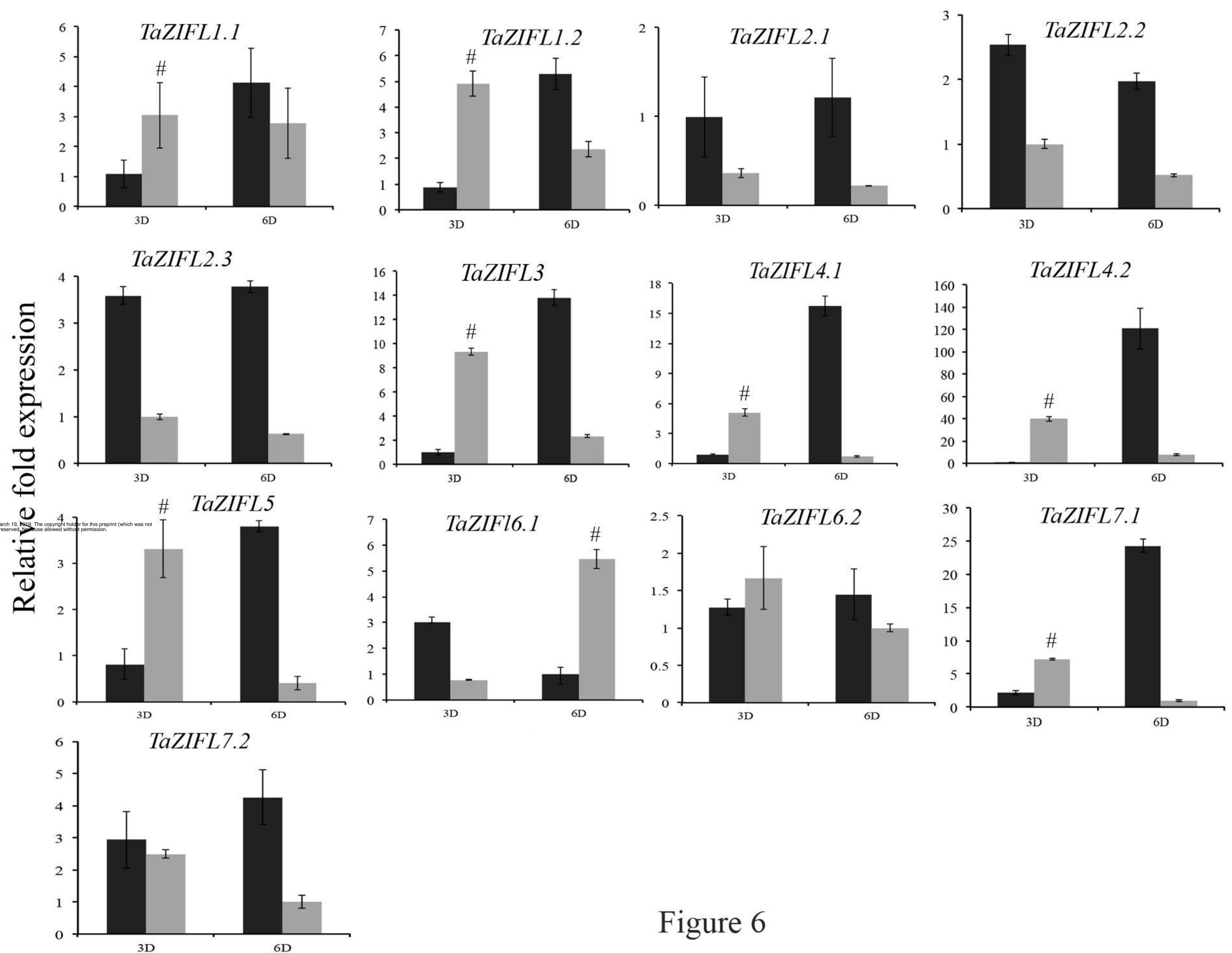


Figure 6

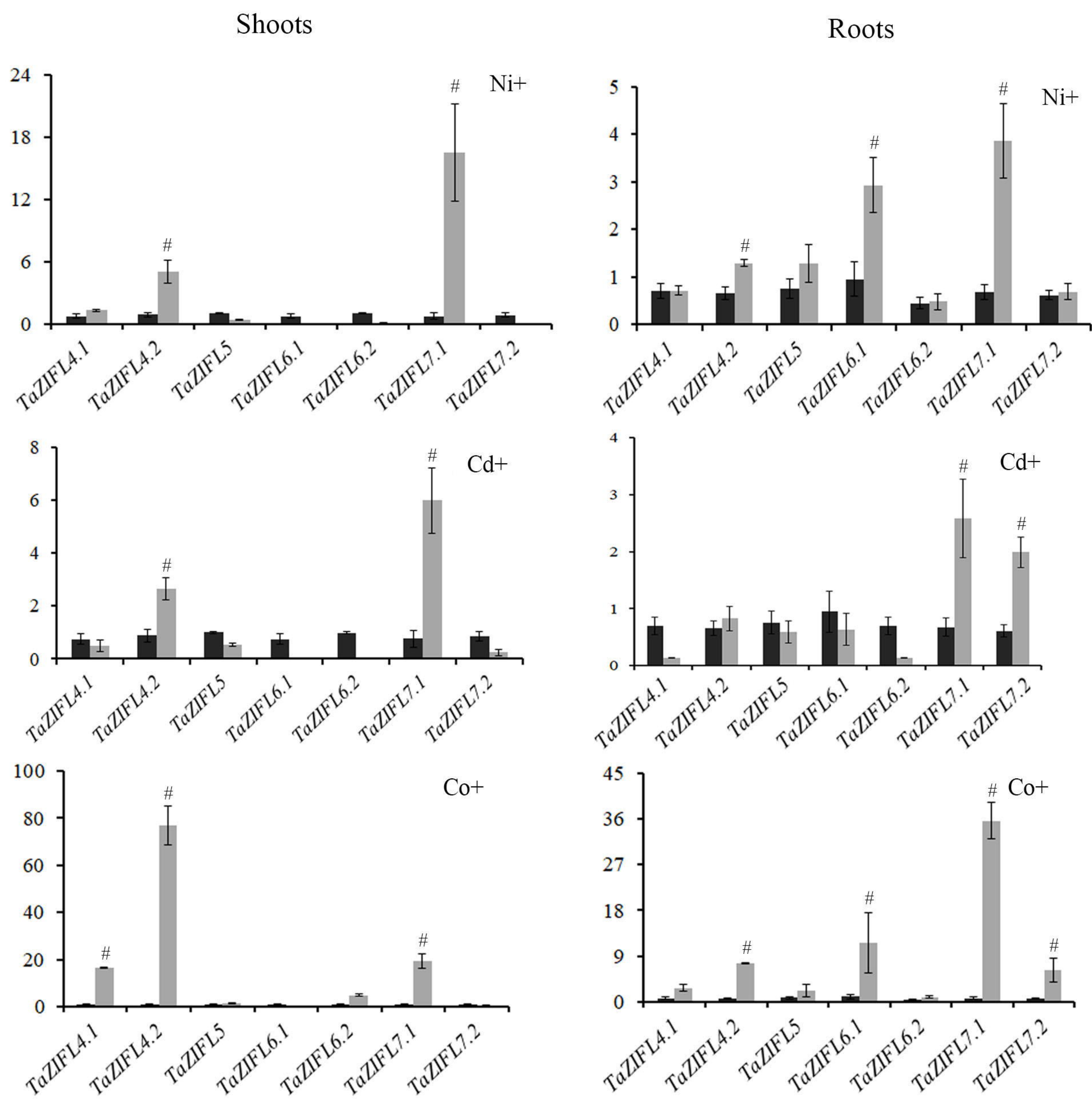


Figure 7

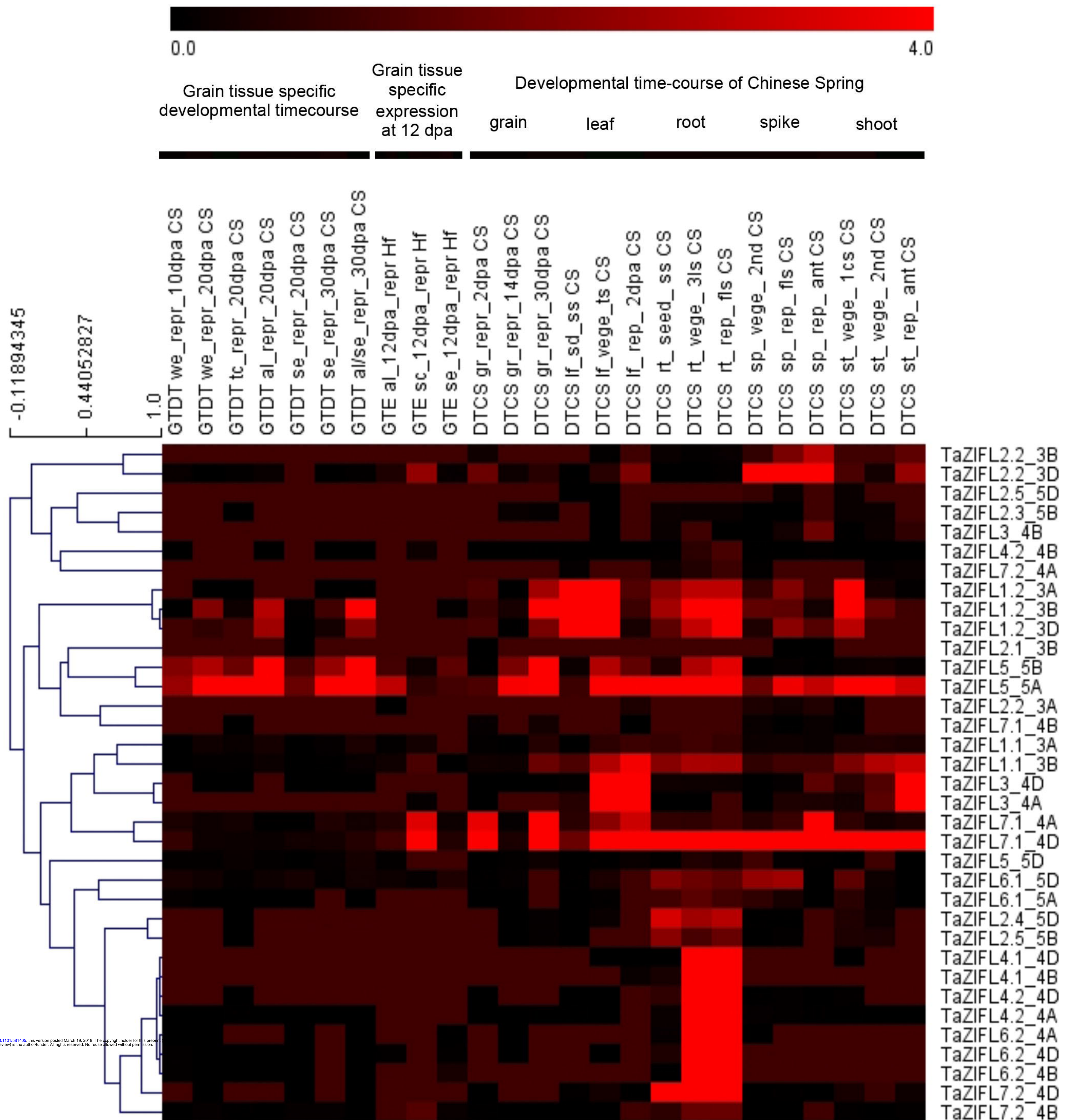


Figure 8